

12th U. S. National Combustion Meeting
Organized by the Central
States Section of the Combustion Institute
May 24–26, 2021(Virtual)
College Station, Texas

Effect of Spray Collapse on Mixture Preparation and Combustion Characteristics of a Spark-Ignition Heavy-Duty Diesel Optical Engine Fueled with Direct-Injected Liquefied Petroleum Gas (LPG)

Rajavasanth Rajasegar^{1,}, Aleš Srna¹*

¹ Combustion Research Facility, Sandia National Laboratories, Livermore, CA, 94550, USA.

* Corresponding author email: rrajase@sandia.gov

Abstract: Liquid Petroleum Gas (LPG), as a common alternative fuel for internal combustion engines is currently widespread in use for fleet vehicles. However, a current majority of the LPG-fueled engines, uses port-fuel injection that offers lower power density when compared to a gasoline engine of equivalent displacement volume. This is due to the lower molecular weight and higher volatility of LPG components that displaces more air in the intake charge due to the larger volume occupied by the gaseous fuel. LPG direct-injection during the closed-valve portion of the cycle can avoid displacement of intake air and can thereby help achieve comparable gasoline-engine power densities. However, under certain engine operating conditions, direct-injection sprays can collapse and lead to sub-optimal fuel-air mixing, wall-wetting, incomplete combustion, and increased pollutant emissions. Direct-injection LPG, owing to its thermo-physical properties is more prone to spray collapse than gasoline sprays. However, the impact of spray collapse for high-volatility LPG on mixture preparation and subsequent combustion is not fully understood. To this end, direct-injection, laser-spark ignition experiments using propane as a surrogate for LPG under lean and stoichiometric engine operating conditions were carried out in an optically accessible, single cylinder, heavy-duty, diesel engine. A quick-switching parallel propane and iso-octane fuel system allows for easy comparison between the two fuels. Fuel temperature, operating equivalence ratio and injection timing are varied for a parametric study. In addition to combustion characterization using conventional cylinder pressure measurements, optical diagnostics are employed. These include infrared (IR) imaging for quantifying fuel-air mixture homogeneity and high-speed natural luminosity imaging for tracking the spatial and temporal progression of combustion. Imaging of infrared emission from compression-heated fuel does not reveal any significant differences in the signal distribution between collapsing and non-collapsing sprays at the spark timing. Irrespective of coolant temperatures, early injection timing resulted in a homogeneous mixture that lead to repeatable flame evolution with minimal cycle-to-cycle variability for both LPG and iso-octane. However, late injection timing resulted in mixture inhomogeneity and non-isotropic turbulence distribution. Under lean operation with late injection timing, LPG combustion is shown to benefit from a more favorable mixture distribution and flow properties induced by spray collapse. On the other hand, identical operating conditions proved to be detrimental for iso-octane combustion most likely caused by distribution of lean mixtures near the spark location that negatively impact initial flame kernel growth leading to increased cycle-to-cycle variability.

Keywords: LPG combustion, optical engine research, flame kernel growth, spray collapse

1. Introduction

Liquid Petroleum Gas (LPG) is attracting increased attention as a cost-efficient alternative fuel [1] for on-road internal combustion engine applications and is an abundantly available US domestic resource. Historically, the primary market for mobility LPG applications were fleet vehicles and retrofit solutions of existing spark-ignition (SI) light-duty engines, which benefited

from straightforward conversion, reduced emissions and lower operating costs [2]. Nevertheless, these outdated powertrains utilizing port fuel-injection and simple engine control systems were unable to exploit the excellent knock resistance of LPG to increase efficiency and usually suffered from a power-loss due to the displacement of intake air with low molecular weight LPG fuel [3]. However, with the development of modern direct-injection engines with direct fuel-injection, high rates of exhaust gas recirculation (EGR), high compression ratio and modern engine control, LPG engine applications are able to reach unprecedented efficiency levels comparable to diesel engine counterparts [4]. Such benefits have been successfully demonstrated for both light- and heavy-duty powertrains.

Despite the success of early DI engine applications, it is likely that considerable optimization potential remains unexploited due to the lacking of science-based understanding of propane direct-injection spray characteristics and combustion behavior under engine relevant conditions. The vapor pressure of LPG's main constituent, propane (min. 96% in the US-market LPG) is about 10 bar at room temperature, which is about one to two orders of magnitude higher than the vapor pressure of commercial gasoline [5]. This makes LPG highly prone to flash-boiling when directly injected into the cylinder [6]. Flash boiling is an important factor driving the spray collapse in a multi-hole, gasoline direct-injection (GDI) injector. Spray collapse is the phenomenon, in which multiple sprays with a wide included angle collapse into a single fuel-spray with a narrow angle [6, 7]. Indeed, several optical studies of LPG injection in constant volume chambers have demonstrated the high propensity of propane sprays to collapse [7-9]. And in the gasoline engine counterparts, spray collapse has been associated with increased wall wetting, changes in mixture formation and increased engine emissions [10, 11]. Therefore, advanced LPG engines may require a re-design of existing GDI injectors to achieve an ideal fuel-air mixture distribution for the best engine performance.

Another largely unexplored aspect of LPG engine applications is the combustion properties of LPG. Aside from the excellent knock resistance and marginally higher laminar flame speeds of LPG when compared to commercial gasoline, several researchers have also reported improved combustion stability and higher tolerance to increased charge dilution with EGR when operating with LPG compared to conventional gasoline [3, 12, 13]. The underlying mechanisms behind these observations are largely unexplored and it is unclear to what extent these observations are indeed related to the spray characteristics of LPG.

The aim of this work is to further the understanding of LPG spray characteristics and its influence on subsequent fuel-air mixture formation and combustion in a single-cylinder, heavy-duty, optical diesel engine. LPG fuel spray collapse and end-of-compression fuel distribution (based on IR emission) are characterized for various injection timings and compared to the reference case of iso-octane used as gasoline surrogate. Furthermore, the engine thermodynamic performance and early flame-kernel development are investigated and correlated to fuel-spray characteristics.

2. Experimental Overview

2.1. Sandia Heavy-Duty Optical Diesel Engine

The experiments were carried out in the Sandia-Cummins single-cylinder, heavy-duty, optical engine, which is a modified version of the single-cylinder Cummins N-series, direct-injection,

heavy-duty, diesel engine. The optical engine has a 13.97-cm bore and 15.24-cm stroke, yielding a displacement of 2.34 L per cylinder. The intake port geometry of the production engine, which has a steady-state (i.e., measured on a flow-bench) swirl ratio of 0.5, is preserved in the optical engine. The engine is equipped with a Bowditch piston with an open, right-cylindrical bowl and a flat fused-silica piston-crown window to allow optical access to the bowl, viewing from below. Flat rectangular windows installed in a ring at the top of the cylinder liner provide additional optical access through the cylinder wall – the piston bowl-rim is interrupted with cutouts at positions matching the window locations to allow camera and laser-access into the combustion chamber through the liner window. Further, one of the two exhaust valves has been replaced with a window, and a periscope mirror in the rocker box gives a view of the squish region (i.e., the region above the piston bowl-rim, not used in this study). Further details about this engine can be found elsewhere [14, 15]. A schematic layout of the optical engine with the imaging setups are shown in Figure 1 and the major specifications of the engine are tabulated in Table 1.

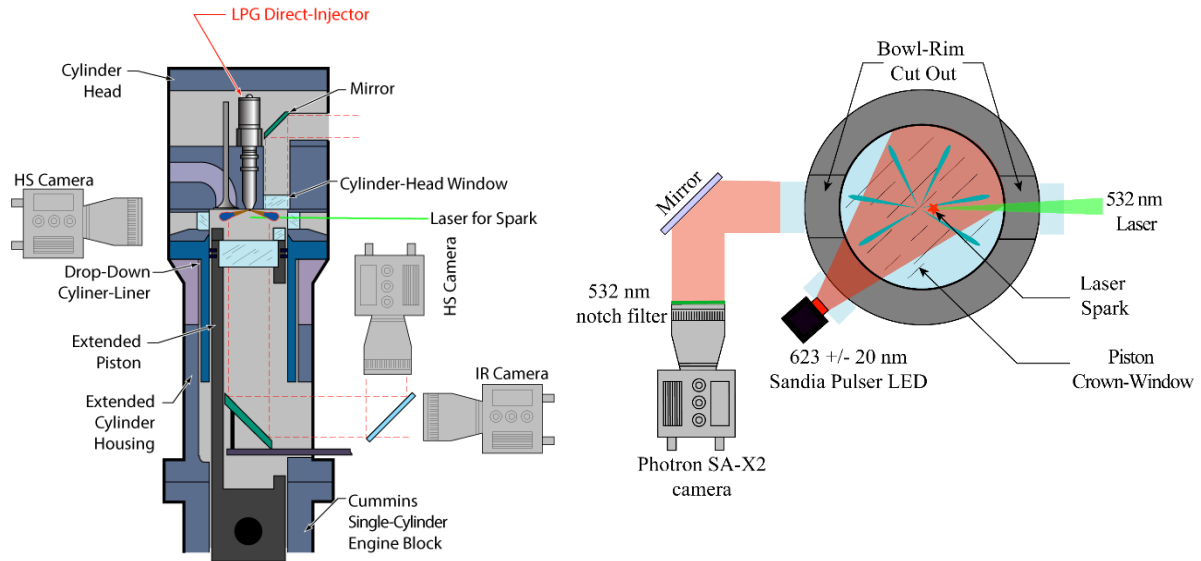


Figure 1: Schematic layout of the optical engine and the imaging setup (left); optical and laser access across the combustion chamber (right).

2.2. LPG Fuel Injection and Ignition systems

A centrally mounted, six-hole, asymmetric, light-duty, gasoline direct injector (GDI) from Bosch was used to inject LPG or iso-octane at an injection pressure of 100 bar. The six injector holes are arranged with roughly a 50° azimuthal spacing leaving about 1/4 of the combustion chamber not targeted by any of the fuel-jets. Such an asymmetric injector hole-design has been shown to decrease the tendency of spray collapse. The steady injection rate for this injector at 100 bar, interpolated from injected mass at different durations of solenoid energizing (DSE), is about 5.8 - 7.6 g/s for LPG (dependent on coolant temperature) and about 8.4 g/s for iso-octane (independent of coolant temperature).

The compressed in-cylinder charge was ignited with a laser-induced spark at 350 crank-angle degrees (CAD) with 360 CAD defined as top dead-center (TDC) of the compression stroke. Laser-spark ignition was selected over conventional spark-plug ignition to avoid extensive modifications

of the engine cylinder head necessary to install a spark-plug in addition to the centrally-mounted injector. The spark location was fixed to be around 10 mm below the fire deck and about 10 mm radially offset from the cylinder axis. The laser energy at 532 nm was adjusted to be 240 mJ/pulse before entering a series of beam-shaping uncoated optical elements, which reduced the energy of the laser beam at the spark location to about 150 mJ/pulse.

2.3. Optical Diagnostics Setup

The optical diagnostics setup consists of a two-view combined Mie-scattering and natural-luminosity (NL) high-speed imaging and bottom view high-speed IR imaging. The Mie/NL imaging system (shown in Figure 1) consists of a pulsed LED (623 nm \pm 20 nm) for spray illumination and two high-speed cameras (Photron FastCam SA-X2) that detect the Mie-scattered light during the fuel-injection and natural flame luminosity during the combustion phase of the cycle. Cameras were synchronized to the engine rotation to acquire one image every $\frac{1}{4}$ degrees crank angle ($^{\circ}$ CA) (14.4 kfps) and acquired images for 100 $^{\circ}$ CA during the injection phase and 50 $^{\circ}$ CA during the combustion phase. The imaging resolution was about 0.14mm/pixel for the bottom view (Nikkor 105 mm f/2.5 glass lens) and 0.08 mm/pixel for the side view (UV-Nikkor 105 mm f/4.5). The side-view camera was equipped with a 532 nm notch filter to block the laser light used for spark-ignition.

The high-speed IR images were acquired at a 2 $^{\circ}$ CA resolution (1800 fps) from the start of injector solenoid energizing until 50 $^{\circ}$ CA after the spark timing with a resolution of about 0.5mm/pixel. The IR camera (FLIR X6900sc) was equipped with a 3.4 μ m (\pm 0.1 μ m) band-pass filter to isolate the C-H stretch IR emission from compression heated hydrocarbons. This method offers line-of-sight averaged information about the distribution of hydrocarbons in the combustion chamber as further described elsewhere [16].

2.4. Engine Operating Conditions and Test Matrix

The engine was operated at 600 RPM with no throttling (1 bar inlet pressure) using inlet air heated to 60 $^{\circ}$ C with no EGR. This relatively slow engine rotation speed was selected in order to allow sufficient time for fuel-injection - the injector's low flow rate for this engine size necessitates long injection durations (up to 100 $^{\circ}$ CA with propane), which would become prohibitive at higher engine speeds. The spark timing was fixed at 350 CAD (10 CAD before TDC) based on a preliminary study involving varying spark timings. This selected spark timing ensures early combustion phasing (CA50 roughly at about 370 CAD) for optimal engine efficiency while avoiding abnormal combustion phenomena like knock.

Test cases involving LPG (propane) were operated with hot and cold engine coolant conditions (coolant temperature determines the fuel temperature at injection) to assess the influence of higher vapor pressure of LPG under hot conditions, whereas the iso-octane test cases were only operated at cold coolant conditions for reference. Both fuels were tested under stoichiometric conditions as well as in lean operation, which is expected to be more sensitive to changes in fuel-air mixing. Furthermore, three injection timings were tested – an early injection during the intake stroke, an intermediate injection and a late injection into the high density ambient conditions, where the injection timing was selected, so that the charge reaches ECN Spray G conditions (573 K, 6 bar, 3.5 kg/m³) at the end of injection (ESE – end of solenoid energizing). Higher charge pressure under late injection conditions is expected to suppress spray collapse.

Engine Specifications			
Engine base type	Cummins N-14, DI diesel		
Combustion Chamber	Quiescent, direct injection		
Swirl ratio	0.5		
Bore \times Stroke [cm]	13.97×15.24		
Bowl Width, Depth [cm]	9.78, 1.55		
Displacement [liters]	2.34		
Compression ratio [-]	10.32		
GDI Injector Specifications			
Fuel injector type	Gasoline direct-injection, Bosch		
Number of holes	6, asymmetric pattern		
Fuel	Propane or iso-octane		
Flow-rate [g/s]	5.8 - 7.6 (propane, fuel-temperature dependent) 8.4 (iso-octane, independent of fuel temperature)		
Operating conditions			
Engine speed [RPM]	600		
Intake charge temperature [°C]	60		
Intake O ₂ [%] (N ₂ dil.)	21		
Intake pressure [bar]	1.0		
Spark timing [CAD]	350		
Fuel	Coolant / Oil	EQR ϕ	Injection timing
LPG	Cold (30°C)	1.0 0.7	Early (SSE = 60 CAD)
	Hot (90°C)		Late (ESE = 311 CAD)
Iso-octane	Cold (30°C)		Intermediate (SSE ~ 120 CAD, $\phi = 0.7$ only)

Table 1. Engine and combustion system specifications and operating conditions.

2.5. Natural Luminosity Image Processing

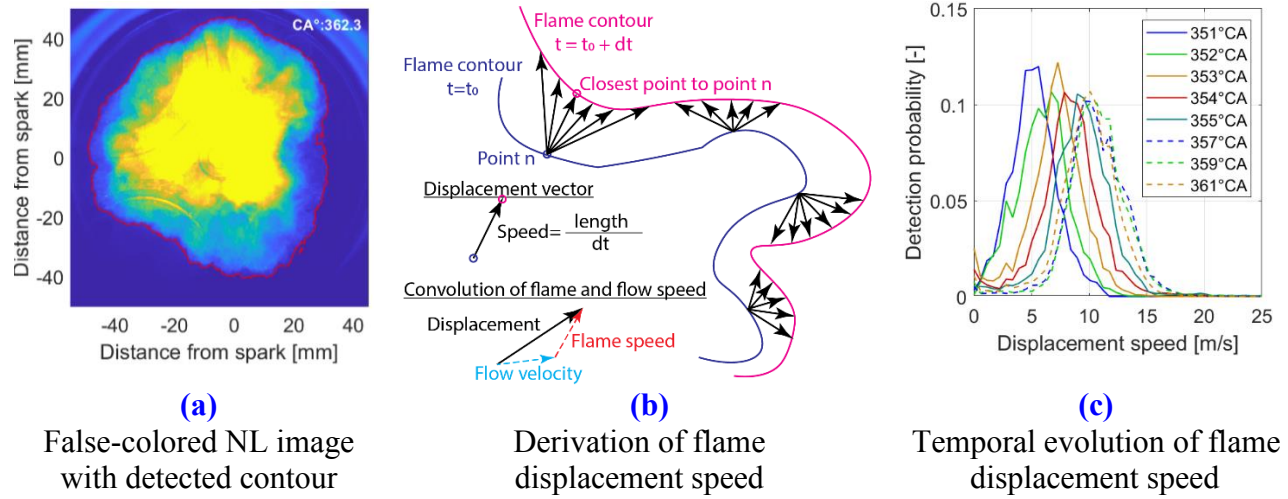


Figure 2: Overview of NL image processing approach to derive the flame contour temporal evolution and the statistics of flame displacement speed.

The natural luminosity images were further processed to enable quantification and comparison of the early flame-kernel development between the cases of the test matrix. First, the flame contour was detected from the NL images as demonstrated in Figure 2.(a) using a in-house developed algorithm that was capable of distinguishing the flame area from other image features with elevated intensity caused by the back-wall reflections or other features of the cylinder head which may appear brighter but are not yet burning.

In the second step, the flame displacement speed is determined. In this study, the flame displacement speed is determined as the ratio of the length, the flame travels between the image frames divided by the inter-frame time as sketched in Figure 2.(b). For each point on the flame contour detected at time $t = t_0$, the closest point on the contour at time $t = t_0 + dt$ is determined. These two points determine the displacement vector, whose length divided by dt gives the displacement speed, which is a convolution of the actual flame speed and flame convection due to the in-cylinder charge motion.

The statistics obtained by analyzing the displacement speed along every point on the contour at various times after ignition, ensemble averaged over the 30 cycles acquired for every operating condition, are finally assembled into a displacement-speed probability density function (PDF) for comparison with other conditions as shown in Figure 2. (c). The displacement speed steadily increases after ignition until it reaches a steady value about 5-6 °CA after ignition. This is mostly likely due to a combination of the large stretch and curvature, the early kernel experiences or due to the increased charge temperature and associated laminar flame speed increase caused by ongoing charge compression and combustion.

3. LPG and Iso-octane Fuel Spray and Mixing Characteristics

3.1. Fuel Spray Evolution

For the purpose of this study, the fuel spray is classified as either collapsed or non-collapsed spray based on the spray cone angle. The collapsed spray is clearly distinguishable from non-collapsed spray which allows for this simple classification by monitoring the Mie-scattering recordings. The LPG spray with early injection collapses within 1 °CA from the start of injection and remains collapsed throughout the injection, regardless of the coolant temperature. On the other hand, the iso-octane spray does not collapse under early injection conditions. The spray evolution during the transient late injection conditions is less steady, as visualized by the image panels at select timings (see Figure 3). The first panel shows LPG sprays, 2 °CA after the start of injection, when the spray is already fully collapsed. During compression, the in-cylinder pressure increase causes the LPG spray to exhibit initial widening of the cone angle (second panel) and finally overcomes spray collapse (significant widening) when the in-cylinder pressure reaches about 2.5 bar. Afterwards, the spray remains fully open until the end of injection (last panel, 5 °CA before end of injection). It is interesting to note that the hot-coolant, late-injection LPG case overcomes spray collapse at the same pressure threshold, despite an order of magnitude higher vapor pressure due to the elevated fuel temperature. On the other hand, the iso-octane spray (Figure 3, right) remains non-collapsed over the entire injection duration. The only apparent difference is the extent of the liquid part of the spray which reduces with increasing pressure and temperature as expected due to faster evaporation. Since the spray pattern is likely to influence the fuel-air mixing and the in-cylinder flow and thereby influence the subsequent combustion process, the spray behavior for all operating conditions is summarized in Table 2 for reference in the following sections.

Table 2: Summary of spray behavior at tested operating conditions.

Fuel	Cold, early inj.	Hot, early inj.	Cold, late inj.	Hot, late inj.
LPG	Full collapse	Full collapse	Recover from collapse at $p > 2.5$ bar	Recover from collapse at $p > 2.5$ bar
Iso-octane	No collapse	N/A	No collapse	N/A

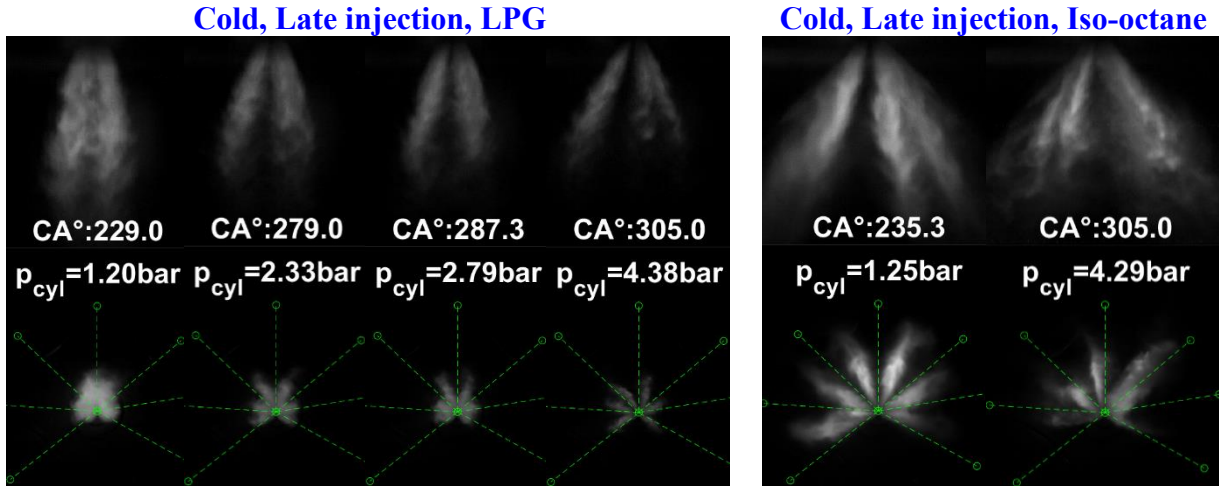


Figure 3: Sample Mie-scattering images of LPG (left) and iso-octane (right) late-injection sprays at key time instants as indicated by the crank angle timings. Side view on the top and bottom view below. The green lines on bottom view separate the azimuthal regions targeted by each nozzle hole.

3.2. Fuel Mixing Characterization

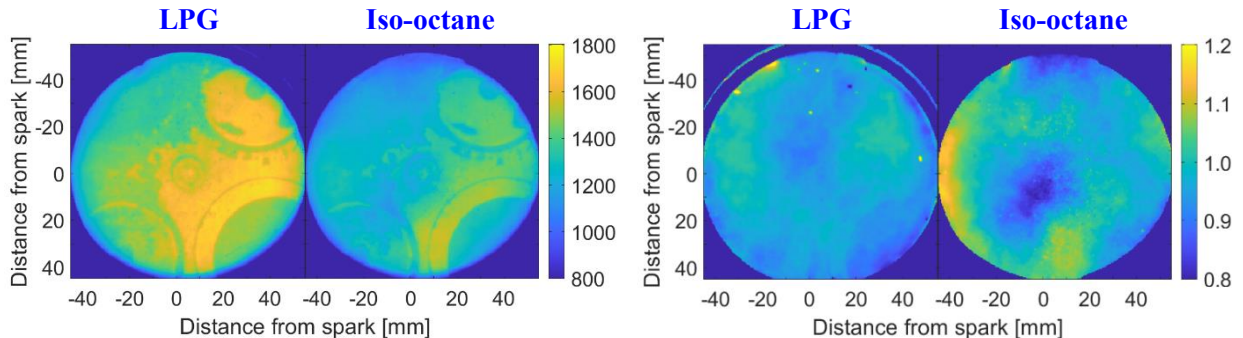


Figure 4: Sample ensemble averaged IR images at 348 CAD (left) and ratio images of IR emission of late-injection over early-injection to reveal potential mixture inhomogeneity for late injections (right).

The hydrocarbon IR emission signal intensity is strongly dependent both on fuel concentration and temperature. Furthermore, as visualized by the ensemble-averaged IR images presented in Figure 4 (left), the IR signal distribution is strongly dominated by reflections from various cylinder head features as well as by vignetting effects which make any quantification impractical. Nevertheless, the ratio of IR signal intensity recorded at a specific timing under an operating point

of interest, divided by the reference image (early injection case) can reveal repeatable differences in the IR signal distribution (Figure 4, right). While the ratio image for LPG shows a fairly uniform signal distribution, in the case of iso-octane, a consistently lower IR emission is detected in the center of combustion chamber, near the spark location. This is most likely due to a combination of the late injection causing a delayed fuel vaporization cooling effect and the non-collapsing spray behavior of iso-octane as discussed earlier and might have further implications on the subsequent combustion behavior as discussed in the following sections.

4. Combustion Characteristics

4.1. Thermodynamic Engine Performance

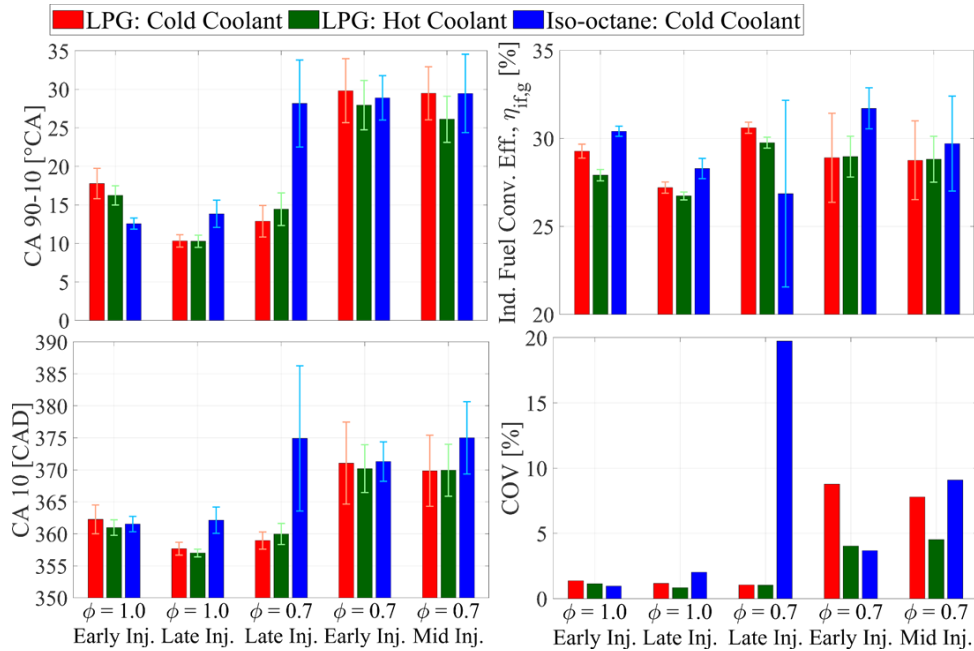


Figure 5: Comparison of engine thermodynamic performance in terms of combustion duration (CA90 - CA10), indicated engine efficiency, CA10 and coefficient of variation (COV).

The thermodynamic engine performance for all the test cases is compared by means of four key metrics in Figure 5. The metrics of duration of initial flame kernel growth (CA10, 10% energy conversion point) and combustion duration (CA90 - CA10) show a large disparity between the lean and stoichiometric operating conditions, with the latter showing faster flame kernel growth and shorter combustion duration, as expected. Despite the slower combustion, the lean operating conditions achieved comparable or higher efficiency than the stoichiometric operation. This is most likely attributed to a more favorable specific heat ratio and reduced heat losses under lean operation as well as later combustion phasing, which might be beneficial at the low engine speeds used in this study.

Nevertheless, deviations from these general trends are observed when comparing late and early injection cases under nominally same conditions, and when comparing LPG and iso-octane cases with late injection. In general, late injection cases with LPG exhibit faster combustion with reduced coefficient of variation (COV) than similar cases with early injection. This is most noticeable under

lean operation that suggests favorable mixture distribution and flow conditions near the spark for fast combustion evolution as further discussed below. Counter-intuitively, late injection cases under stoichiometric operation show inferior engine efficiency, which is most likely due to mixing-related incomplete combustion or sub-optimal combustion phasing. Nevertheless, different trends are observed for iso-octane cases. Under stoichiometric operation, the injection timing has a negligible influence on iso-octane combustion, while for lean operation the late injection timing proved to be highly detrimental for iso-octane as slow combustion evolution with frequent misfires was observed. These trends are further discussed in the following sections employing optical diagnostics.

4.2. Influence of Injection Timing

The influence of LPG injection timing on the combustion evolution for stoichiometric operation is visualized by comparing the flame contour temporal evolution for 5 representative cycles (CA10 closest to the average value) in the left panel of Figure 6. The line-style identifies the cycle while the line-color marks the time in the cycle. The change in injection timing reduces the available time for mixing and dissipation of the injection-generated turbulence and flow motion which likely leads to less homogenous and more turbulent charge for the late injections. Furthermore, as discussed in Section 3, the LPG spray remains fully collapsed during the early injection phase; while, after initial spray collapse, the spray overcomes the collapse during the last-third of the injection period, when the in-cylinder pressure exceeds 3-5 bar. As seen from Figure 6, the early flame kernel evolution is stable and repeatable for both injection cases, nevertheless, much faster flame evolution is detected for late injection timing, consistent with increased turbulence, alongside a repeatable deflection of the flame kernel towards upper-right side of combustion chamber. This deflection most likely suggests the existence of a repeatable bulk-flow motion or a mixture inhomogeneity in the combustion chamber that creates a preferential direction for flame propagation.

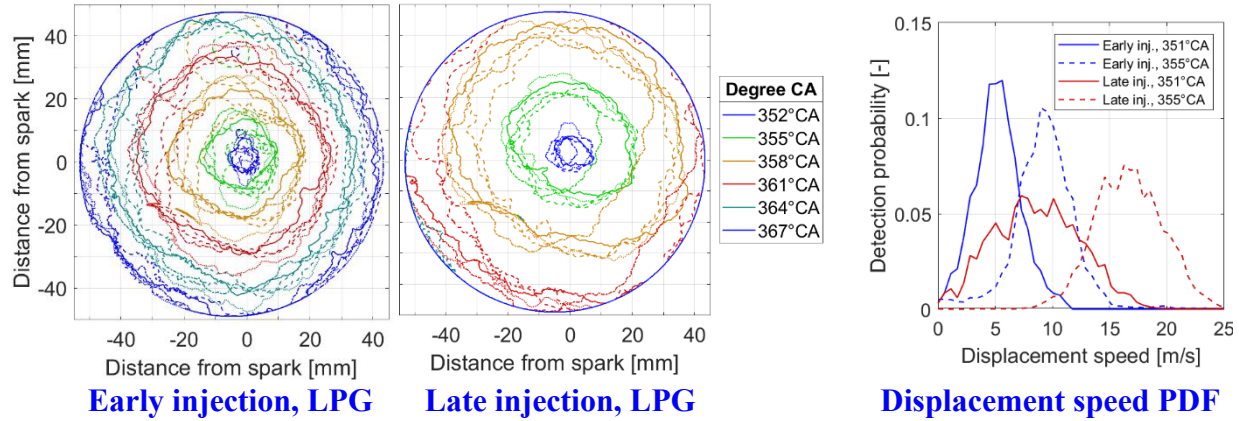


Figure 6: Temporal evolution of the flame contours (left and middle) for 5 representative cycles under stoichiometric operation ($\phi = 1.0$, LPG) along with flame displacement speed statistics (right).

The late-injection displacement speed exceeds the early-injection statistics by roughly a factor of 2. Initially after ignition, the late-injection, flame displacement speed PDF is much broader consistent with large-scale eddy-motion deflecting the flame kernel which, when convoluted with

the actual flame speed, results in a wide distribution. On the other hand, with early injection, the PDF remains rather narrow at both presented timings, consistent with the expectation of a more quiescent charge. The displacement speed in both cases considerably exceeds the burnt-side laminar flame speed, which is on the order of 3 m/s for both fuels under conditions around the spark timing. This indicates the presence of considerable flame acceleration due to turbulence, even with the early injection.

4.3. Lean Operation

Lean operation conditions are expected to further emphasize the potential mixture inhomogeneity effects. Indeed, the representative flame contours on Figure 7 show considerable differences in the flame evolution between the early and late injection cases. The latter shows similar evolution to stoichiometric operation though with a more pronounced flame deflection towards the upper-right side of the view, indicating the same bulk-flow motion and/or mixture inhomogeneity persists under lean conditions as well. The flame kernel evolution reveals considerable cyclic variability despite the similar CA10 values (only reached at about 371 CAD), which confirms the high sensitivity of combustion to local flow and mixture inhomogeneity. It appears likely that some degree of mixing inhomogeneity exists in both cases. This is indicated by the high probability of near-zero flame displacement speeds detected in the early injection case (Figure 7, right) and the broad PDF in late-injection case. The near-zero flame displacement speeds correlate to a slow lean flame that cannot resist deflection by the flow while the broader PDF for late injection indicates both slow-burning zones as well as fuel-richer zones that reach 80% of the maximal flame displacement speeds detected under stoichiometric conditions despite the 50% reduction in laminar flame speed.

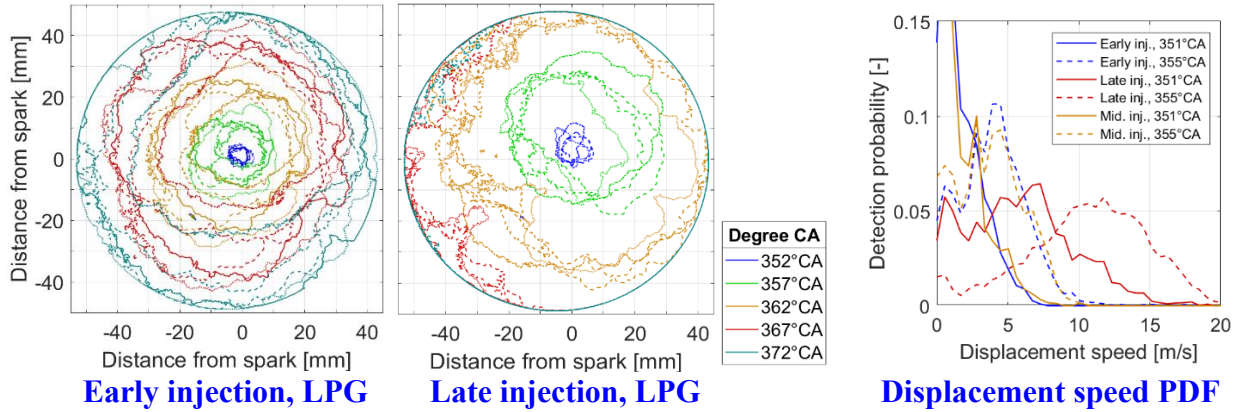


Figure 7: Temporal evolution of the flame contours (left and middle) for 5 representative cycles under lean operation ($\phi = 0.7$, LPG) along with flame displacement speed statistics (right).

4.4. Comparison of Stoichiometric Late-injection LPG and Iso-octane

The difference between iso-octane and LPG is primarily in the spray behavior. Iso-octane sprays do not collapse under any conditions in this study and has about a 15% reduced laminar flame speed when compared to LPG. Despite the nearly indistinguishable performance under early injection conditions, the late injection cases reveal stark differences between the two fuels. Iso-octane exhibits around 50% slower early flame-kernel evolution when compared to LPG (see

Figure 8) and poor repeatability of early kernel evolution. Furthermore, the end-of-compression flow field appears to have been changed since the iso-octane cases do not show the same deflection of early flame kernel as observed with LPG. Considering the comparable performance with early injection, the reduced laminar flame speed is unlikely to have been the underlying cause for the observed differences. While it cannot be excluded that under lean operation, the differences in flame speed between the two fuels might contribute to the difference in performance, the modified mixture distribution and flow-field due to the distinctly different spray behavior appears more likely to be the dominant cause for the observed differences among the two tested fuels.

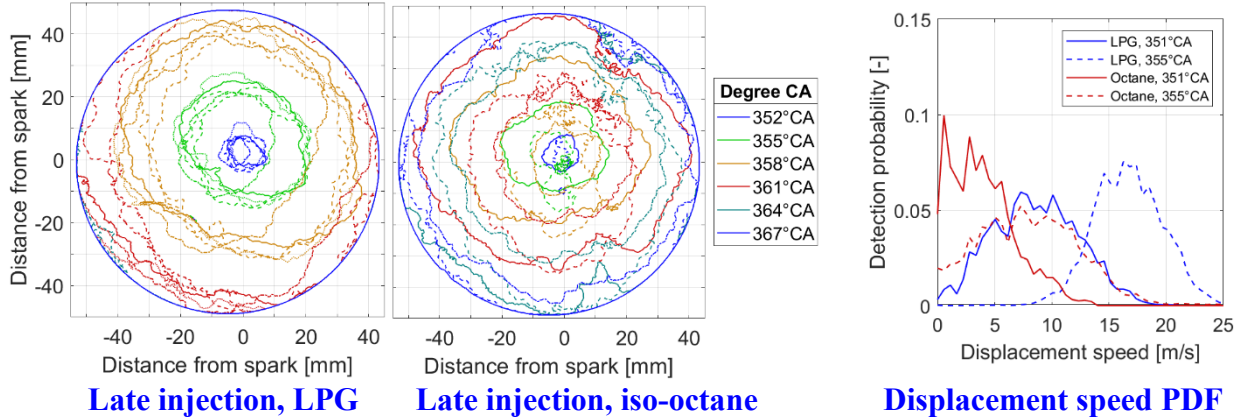


Figure 8: Temporal evolution of the flame contours for 5 representative cycles under stoichiometric operation ($\phi=1$, LPG (left) and iso-octane (middle) and the flame displacement speed statistics (right)

5. Summary and Conclusions

This study investigated the spray characteristics of propane (LPG surrogate) direct-injection and combustion in a heavy-duty, optical, diesel engine equipped with light-duty, automotive, gasoline, direct-injector and laser-spark ignition. Propane combustion cases were compared to reference cases injecting iso-octane used as a gasoline surrogate to elucidate the role of fuel-spray collapse and fuel-properties on the engine thermodynamic performance. High-speed Mie-scattering imaging and IR imaging were employed to characterize the fuel-spray behavior and subsequent fuel-air mixing while high-speed natural-luminosity imaging offered insight into the early flame kernel evolution. Positive correlation between spray collapse and modified end-of-compression mixture distribution and flow-field was identified, which was found to further influence the early flame evolution and engine thermodynamic performance as summarized below:

1. The high-vapor pressure of propane induces a spray collapse in case of early injection at all tested coolant temperatures. In the case of late injections, with the commercial GDI injector, the LPG spray overcomes spray collapse when the in-cylinder pressure exceeds a threshold of about 3-5 bar. Surprisingly, this threshold appears to be rather independent of fuel temperature.
2. Ensemble-averaged IR images show a fairly-homogeneous fuel mixture distribution for all tested conditions. Nevertheless, minor variations in the IR intensity indicate that when

Subtopic: Internal Combustion Engines

injecting late, the injection of LPG relative to iso-octane, resulted in a higher fuel concentration near the spark location in the center of combustion chamber.

3. Spray collapse has no observable influence on combustion characteristics when injecting early during the intake stroke. This is likely associated with the early injection allowing sufficient time for mixing and dissipation of injection-induced flow patterns.
4. Late injection flow and flame-kernel evolution are dissimilar between LPG and iso-octane fuels. A tumble-like flow motion and faster, more repeatable combustion were observed for LPG compared to iso-octane under nominally similar conditions. This highlights the importance of injection-induced flow under late-injection conditions.
5. The dissimilarity in performance of LPG and iso-octane under late-injection condition is further emphasized under lean operation. While combustion with LPG remains fast and stable, iso-octane suffers from slow combustion and ignition-difficulties leading to frequent misfires. The differences in fuel-air mixing partly can explain these observations; nevertheless, the previously reported higher tolerance of LPG to dilution compared to gasoline fuels might additionally amplify this behavior.

Further research is necessary to better separate the flow-field effects induced by the spray characteristics from the mixture inhomogeneity and general combustion related properties of the fuels like the sensitivity to dilution and lean operation. High-fidelity laser based optical diagnostics can be used to characterize the fuel-air mixing. Further test-rig modifications are necessary to achieve in-cylinder flow conditions more representative of modern SI engines and to further study the fuel sensitivity to dilution – this can be achieved by artificial in-cylinder tumble generation (air-injection to generate tumbling motion) or by using a turbulent-jet ignition system that are commonly employed in diesel-engine-derived lean-burning natural gas engines.

6. Acknowledgments

This research was sponsored by the U.S. Department of Energy (DOE) Office of Energy Efficiency and Renewable Energy (EERE). Optical engine experiments were conducted at the Combustion Research Facility (CRF), Sandia National Laboratories (SNL), Livermore, CA. Sandia National Laboratories is a multi-mission laboratory managed and operated by National Technology and Engineering Solutions of Sandia, LLC., a wholly owned subsidiary of Honeywell International, Inc., for the U.S. Department of Energy's National Nuclear Security Administration (NNSA) under contract DE-NA0003525. The authors gratefully acknowledge fruitful discussions with Mark Musculus and the contributions of Dave Cicone for his assistance in maintaining the research engine used in this study.

7. References

1. Raslavičius, L., et al., *Liquefied petroleum gas (LPG) as a medium-term option in the transition to sustainable fuels and transport*. Renewable and Sustainable Energy Reviews, 2014. **32**: p. 513-525.
2. MacLean, H.L. and L.B. Lave, *Evaluating automobile fuel/propulsion system technologies*. Progress in Energy and Combustion Science, 2003. **29**(1): p. 1-69.

Subtopic: Internal Combustion Engines

3. Bayraktar, H. and O. Durgun, *Investigating the effects of LPG on spark ignition engine combustion and performance*. Energy Conversion and Management, 2005. **46**(13): p. 2317-2333.
4. Myung, C.-L., et al., *Comparative study of engine control strategies for particulate emissions from direct injection light-duty vehicle fueled with gasoline and liquid phase liquefied petroleum gas (LPG)*. Fuel, 2012. **94**: p. 348-355.
5. Williams, M.L., *CRC Handbook of Chemistry and Physics, 76th edition*. Occupational and Environmental Medicine, 1996. **53**(7): p. 504.
6. Zhang, Z., et al., *Characteristics of trans-critical propane spray discharged from multi-hole GDI injector*. Experimental Thermal and Fluid Science, 2018. **99**: p. 446-457.
7. Lacey, J., et al., *Generalizing the behavior of flash-boiling, plume interaction and spray collapse for multi-hole, direct injection*. Fuel, 2017. **200**: p. 345-356.
8. Sphicas, P., et al., *Inter-plume aerodynamics for gasoline spray collapse*. International Journal of Engine Research, 2017. **19**(10): p. 1048-1067.
9. Wu, S., et al., *Near-nozzle spray and spray collapse characteristics of spark-ignition direct-injection fuel injectors under sub-cooled and superheated conditions*. Fuel, 2016. **183**: p. 322-334.
10. Yang, J., et al., *Influence of flash boiling spray on the combustion characteristics of a spark-ignition direct-injection optical engine under cold start*. Combustion and Flame, 2018. **188**: p. 66-76.
11. Mohd Murad, S.H., et al., *Spray Behaviour and Particulate Matter Emissions with M15 Methanol/Gasoline Blends in a GDI Engine*. 2016, SAE International.
12. Kim, T.Y., et al., *The effects of stratified lean combustion and exhaust gas recirculation on combustion and emission characteristics of an LPG direct injection engine*. Energy, 2016. **115**: p. 386-396.
13. Lee, K. and J. Ryu, *An experimental study of the flame propagation and combustion characteristics of LPG fuel*. Fuel, 2005. **84**(9): p. 1116-1127.
14. Niki, Y., et al., *Verification of diesel spray ignition phenomenon in dual-fuel diesel-piloted premixed natural gas engine*. International Journal of Engine Research. **0**(0): p. 1468087420983060.
15. Rajasegar, R., et al., *Influence of pilot-fuel mixing on the spatio-temporal progression of two-stage autoignition of diesel-sprays in low-reactivity ambient fuel-air mixture*. Proceedings of the Combustion Institute, 2021. **38**(4): p. 5741-5750.
16. Rajasegar, R., et al., *Spatio-Temporal Progression of Two-Stage Autoignition for Diesel Sprays in a Low-Reactivity Ambient: n-Heptane Pilot-Ignited Premixed Natural Gas*. SAE Technical Paper, 2021-01-0525, 2021.